
Anchor Data Augmentation

Nora Schneider¹ Shirin Goshtasbpour^{1,2} Fernando Perez-Cruz^{1,2}

¹Computer Science Department, ETH Zurich, Zurich, Switzerland

²Swiss Data Science Center, Zurich, Switzerland

nschneide@student.ethz.ch
shirin.goshtasbpour@inf.ethz.ch
fernando.perezacruz@sdsc.ethz.ch

Abstract

We propose a novel algorithm for data augmentation in nonlinear over-parametrized regression. Our data augmentation algorithm borrows from the literature on causality and extends the recently proposed Anchor regression (AR) method for data augmentation, which is in contrast to the current state-of-the-art domain-agnostic solutions that rely on the Mixup literature. Our Anchor Data Augmentation (ADA) uses several replicas of the modified samples in AR to provide more training examples, leading to more robust regression predictions. We apply ADA to linear and nonlinear regression problems using neural networks. ADA is competitive with state-of-the-art C-Mixup solutions.¹

1 Introduction

Data augmentation is one of the key ingredients of any successful application of a machine learning classifier. The first example that typically comes to mind is the in-depth description of the data augmentation in the now-famous Alexnet paper [26]. Data augmentation algorithms come in different flavors, and they mostly rely on the expectation that small perturbations, invariances, or symmetries applied to the input will not change the class label. That way, we can present ‘fresh new’ samples as alterations of the available examples for training. These transformations modify the input distribution to make the algorithm more robust for cases where the distribution of the test set may differ from that of the training set. We refer the reader to the related work section (Section 2.1) for an overview and description of different data augmentation strategies.

The literature for data augmentation in regression is slim. The paper on Mixup augmentation [51] proposes a simple and general scheme for data augmentation using convex combinations of samples. The authors only apply their data augmentation proposal to classification problems. They conjecture in the discussion that the application to regression is *straightforward*, however, this is not the case in practice. Mixup is theoretically analyzed in [5, 52] as a regularization technique for classification and regression problems. However, it is only illustrated in classification problems.

The Mixup algorithm has been extended to regression problems in [18, 49], in which the authors explain that Mixup cannot be blindly applied to regression problems. To our knowledge, these are the only two papers in which data augmentation for regression is proposed. RegMix [18] relies on a hard-to-train prior neural network controller before augmenting the data using a Mixup strategy. *C-Mixup* [49], a method proposed more recently, solves some of the issues limiting the standard Mixup algorithm for regression problems. The authors propose to mix only closeby samples in the

¹Our Python implementation of ADA is available at: <https://github.com/noraschneider/anchordataaugmentation/>

output space (i.e., samples which have close enough labels). This strategy is only valid when the target variables are monotonic with the input and is applied in a transformed space. The authors present comprehensive results in data augmentation for in-distribution generalization, task generalization and out-of-distribution robustness.

In this paper, we rely on the causality literature to provide a different avenue for augmenting data in regression problems. Causal discovery finds the causes of a response variable among a given set of observations or helps to recognize the causal relations between a set of variables [39]. These causes allow us to understand how these relations will change if we were to intervene in a subset of the (input) variables or what would be the effect on the output. So, in general, the regression model will be robust to perturbations in the input variables making the prediction less sensitive to changes in the distribution of the test set. For example, the authors in [40] use the invariance property for prediction to perform causal inference. In turn, Anchor Regression (AR) builds upon the causality literature to obtain robust regression solutions when the input variables have been perturbed [42]. The procedure relies on anchor variables capturing the heterogeneity within a dataset and a parameter γ that measures the deviation with respect to the least square solution. Once the values of the anchors are known, AR modifies the data and obtains the least square solution, as detailed in Section 2.2.

In this paper, we propose **Anchor Data Augmentation (ADA)** to augment the training dataset with several replicas of the available data. We use a simple clustering of the data to encode a homogeneous group of observations and use different values of γ to robustify the solution to different strengths of potential distribution shifts. In every minibatch, we sample γ from a predetermined range around $\gamma = 1$. As AR was developed for linear regression, the data augmentation strategy needs to be modified for nonlinear regression accordingly. We validate ADA for in-distribution generalization and out-of-distribution robustness under the same conditions proposed in C-Mixup [49], as well as some illustrative linear and nonlinear regression examples. In the replicated experiments, ADA is competitive or superior to other augmentation strategies such as C-Mixup, although on some datasets the performance gain is marginal.

The rest of the paper is organized as follows: First, we provide background information in Section 2. We give a brief overview of related work on data augmentation in Section 2.1 and summarize the key concepts on Anchor Regression in Section 2.2. Second, Section 3 shows how we extend Anchor Regression and introduces ADA. Section 4 reports empirical evidence that our approach can improve predictions, especially in over-parameterized settings. We conclude the paper in Section 5.

2 Background

2.1 Data Augmentation

Many different data augmentation methods have been proposed in recent years with several applications in mind. Still most augmentations we mention here use human-designed transformations based on domain knowledge which leave the target variable invariant. For instance, Cutout [10] is an image-specific augmentation technique that is successfully used to train models on CIFAR10 and CIFAR100 [25], but was determined to be unsuitable for larger image datasets like ImageNet with higher resolution [9]. Other augmentation methods for images such as random crop, horizontal or vertical mirroring, random rotation, or translation [29, 43] may similarly apply to a certain group of image datasets while being inapplicable to others, e.g. datasets of digits and letters.

In an attempt to automate the augmentation process and reduce human involvement, policy or search-based automated augmentation methods were developed. In AutoAugment [7] a neural network is trained with Reinforcement Learning (RL) to combine an assortment of transformations in varying strengths to apply on samples of a given dataset and improve the model accuracy. Methods such as RandAugment [8], Fast AutoAugment [30], UniformAugment [32] and TrivialAugment [36] aim at reducing the cost of the pretraining search phase in automated augmentation with randomized transformations and reduced search space.

Alternatively, in order to adapt the augmentation policy to the model during training, Population-Based Augmentation [16] and Online Hyperparameter Learning [31] use multiple data augmentation workers that are updated using evolutionary strategies and RL, respectively. Adversarial AutoAugment [53] and AugMax [47] optimize for the augmentation policy that deteriorates the training accuracy

and improves its robustness. DivAug [34] finds the policy which maximizes the diversity of the augmented data.

Having a separate search phase for optimal augmentation policy is computationally expensive and may exceed the required computation to train the downstream model [8, 48]. In addition, these methods and their online counterparts need to be trained separately on every single dataset. While OnlineAugment [44] and DDAS exploit meta-learning to avoid this problem, they still rely on a set of predefined class invariant transformations that require domain-specific information.

Generic transformations such as Gaussian or adversarial noise [10, 28, 45] and dropout [3] are also effective in expanding the training dataset. Generative models such as Generative Adversarial Networks (GAN) [13] and Variational Auto-Encoders (VAE) [22] are trained in [1, 6, 44] to synthesize samples close to the low dimensional manifold of the data for classification.

Mixup [51] is a popular data augmentation using a convex combination of pairs of samples from different classes and their softened labels for augmentation. Mixup is only evaluated on classification problems, even though it is claimed that the application to regression is straightforward. Various extensions of Mixup have been proposed to prevent data manifold intrusion [46], use more complex mixing strategies [33, 50] or account for saliency in augmented samples [20, 21]. These methods were predominantly designed to excel in classification tasks. In particular, Mixup for regression was studied in [5, 18, 49, 52] but it was reported to adversely impact the predictions in regression problems when misleading augmented samples are generated from a pair of faraway samples.

2.2 Anchor Regression

We summarize the key concepts of Anchor Regression (AR) as presented in [42]. Let $X \in \mathcal{X}$ and $y \in \mathcal{Y}$ be the predictors and target variables sampled from distribution $(X, y) \sim P_{\text{train}}$, $\mathcal{X} \subseteq \mathbb{R}^d$ and $\mathcal{Y} \subseteq \mathbb{R}$. Traditionally, a causal framework models the relation of y and X to accurately predict the value of y under given interventions or arbitrary perturbations on X . A commonly held assumption is that the underlying causal relation among variables remains the same while the sampling distribution P_{train} is altered by the intervention shift or the applied perturbation. For instance, if the distribution P_{train} is induced by an unknown linear causal model, then the causally optimal parameters can be expressed as the solution to the optimization problem:

$$b_{\text{causal}} = \arg \min_b \max_{P \in \mathcal{P}} \mathbb{E}_P[(y - X^T b)^2], \quad (1)$$

where \mathcal{P} is the class of distributions containing all interventions on components of X [41]. Therefore, causal parameters provide distributionally robust predictions that are optimal under the intervention in \mathcal{P} . In comparison, Ordinary Least Squares (OLS):

$$b_{\text{OLS}} = \arg \min_b \mathbb{E}_{P_{\text{train}}}[(y - X^T b)^2], \quad (2)$$

may lead to arbitrarily large predictive errors on distributions in \mathcal{P} . On the other hand, on P_{train} , causal parameters b_{causal} lead to conservative predictions, while b_{OLS} presents optimal least squared performance.

To trade-off predictive accuracy on the training distribution with distribution robustness and to enforce stability over statistical parameters, AR [4, 42] proposes to relax the regularization in the optimization problem in (1) to a smaller class of distributions \mathcal{P} .

Assume that X and y are centered and have finite variance. We use $A \in \mathbb{R}^q$ (called anchors) to denote the exogenous (random) variables in X which generate heterogeneity in y . We further denote the L_2 -projection on the linear span of the components of A with P_A and $\text{Id}(y) = y$. Under linear assumption between A and (X, y) , we can write the relaxed optimization problem as:

$$b_{\gamma, A} = \arg \min_b \mathbb{E}_{P_{\text{train}}}[(\text{Id} - P_A)(y - X^T b)^2] + \gamma \mathbb{E}_{P_{\text{train}}}[(P_A(y - X^T b))^2], \quad (3)$$

where $\gamma > 0$ is a hyperparameter. The first term of the AR objective in Equation 3 is the loss after ‘‘partialling out’’ the anchor variable, which refers to first linearly regressing out A from X and y and subsequently using OLS on the residuals. The second term is the well-known estimation objective used in the Instrumental Variable setting [11]. Therefore, for different values of γ AR interpolates between the partialling out objective ($\gamma = 0$) and the IV estimator ($\gamma \rightarrow \infty$) and coincides with

OLS for $\gamma = 1$. The authors show that the solution of AR optimizes a worst-case risk under shift-interventions on anchors up to a given strength. This in turn increases the robustness of the predictions to distribution shifts at the cost of reducing the in-distribution generalization.

In the finite-sample case with n observations from P_{train} , let matrix $\mathbf{X} \in \mathbb{R}^{n \times d}$ contain the observations of X and let $\mathbf{Y} \in \mathbb{R}^n$ be the vector of corresponding targets. Similarly, we denote the matrix containing the observations of A with $\mathbf{A} \in \mathbb{R}^{n \times q}$ and we use $\mathbf{\Pi}_A = \mathbf{A} (\mathbf{A}^T \mathbf{A})^\dagger \mathbf{A}^T$ as the projection operator on the column space of the anchor matrix \mathbf{A} where \mathbf{A}^\dagger denotes the pseudo-inverse of matrix \mathbf{A} . Further, \mathbf{I} denotes the identity matrix. Then, the finite-sample optimization regression problem can be written as

$$\hat{b}_{\gamma, \mathbf{A}} = \arg \min_b \|(\mathbf{I} - \mathbf{\Pi}_A)(\mathbf{Y} - \mathbf{X}b)\|_2^2 + \gamma \|\mathbf{\Pi}_A(\mathbf{Y} - \mathbf{X}b)\|_2^2. \quad (4)$$

The AR regression estimate $\hat{b}_{\gamma, \mathbf{A}}$ can be obtained by applying the OLS solution to a modified set of inputs and outputs:

$$\tilde{\mathbf{X}}_{\gamma, \mathbf{A}} = \mathbf{X} + (\sqrt{\gamma} - 1)\mathbf{\Pi}_A \mathbf{X} \quad (5)$$

$$\tilde{\mathbf{Y}}_{\gamma, \mathbf{A}} = \mathbf{Y} + (\sqrt{\gamma} - 1)\mathbf{\Pi}_A \mathbf{Y} \quad (6)$$

3 Anchor Data Augmentation

In this section, we introduce Anchor Data Augmentation (ADA), a domain-independent data augmentation method inspired by AR. ADA does not require previous knowledge about the data invariances nor manually engineered transformations. As opposed to existing domain-agnostic data augmentation methods [10, 45, 46], we do not require training of an expensive generative model, and the augmentation only adds marginally to the computation complexity of the training. In addition, since ADA originates from a causal regression problem, it can be readily applied to regression problems. Even when ADA does not improve performance, its effect on performance remains minimal.

Data augmentation aims to introduce informative data in addition to the original dataset during the training procedure of the model to improve its generalization. Similar to AR, ADA employs a linear projection, given by the anchor variables A , to determine the most relevant perturbation directions based on the similarity of the samples. ADA inherits the generalization properties from AR. In [42], the authors recommend that the anchor variable can be set as *an indicator of the datasets, where each dataset is a homogeneous set of observations*. A key insight of our work is that this can be achieved by clustering the data into q clusters. The matrix $\mathbf{A} \in \mathbb{R}^{n \times q}$ is then constructed as an indicator matrix with a one-hot encoding of the assigned cluster index per row. For our experiments, we use *k-means* clustering [35] to construct \mathbf{A} . Further, in AR, only one value for γ is used, which should be chosen based on the desired strength of perturbations on test datasets, in comparison to the training dataset [42]. We suggest that the value of γ is sampled from a distribution with density $p(\gamma)$. In our experiments, we use a uniform distribution between $1/\alpha$ and α , where $\alpha > 1$ is a hyperparameter to be tuned.

ADA augments a sample $(\mathbf{X}^{(i)}, \mathbf{Y}^{(i)})$ by normalizing the original AR modifications (5 and 6) by $1 + (\sqrt{\gamma} - 1) \sum_j (\mathbf{\Pi}_A)^{(ij)}$ to unify the noise level across the augmentations independent of the value of γ , while approximately preserving the potentially nonlinear relation between X and y (see also section 3.2):

$$\tilde{\mathbf{X}}_{\gamma, \mathbf{A}}^{(i)} = \frac{\mathbf{X}^{(i)} + (\sqrt{\gamma} - 1)(\mathbf{\Pi}_A)^{(i)} \mathbf{X}}{1 + (\sqrt{\gamma} - 1) \sum_j (\mathbf{\Pi}_A)^{(ij)}}, \quad (7)$$

$$\tilde{\mathbf{Y}}_{\gamma, \mathbf{A}}^{(i)} = \frac{\mathbf{Y}^{(i)} + (\sqrt{\gamma} - 1)(\mathbf{\Pi}_A)^{(i)} \mathbf{Y}}{1 + (\sqrt{\gamma} - 1) \sum_j (\mathbf{\Pi}_A)^{(ij)}}, \quad (8)$$

where we denote $(\mathbf{M})^{(i)}$, $(\mathbf{M})^{(j)}$, and $(\mathbf{M})^{(ij)}$ denote respectively the i -th row, the j -th column and (i, j) component of some matrix \mathbf{M} . As is standard practice, we rely on stochastic gradient descent to optimize our (nonlinear) regressors and apply ADA on each minibatch rather than the entire dataset.

ADA combines samples from the same cluster and generates augmented samples along the data manifold. For a general \mathbf{A} , $\mathbf{\Pi}_A$ provides a ‘‘collective’’ mixing approach for the samples in a batch

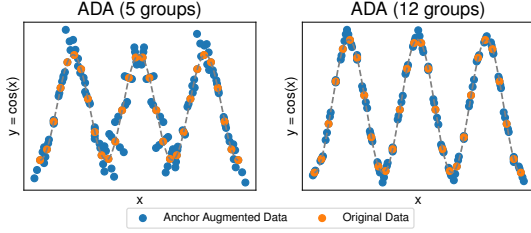


Figure 1: Comparison of ADA augmentations on a nonlinear Cosine data model. For a larger partition size, ADA augmentations are more accurate due to the high local variability of the Cosine function. We used *k-means* clustering to construct \mathbf{A} and $\gamma \in \{1/2, 2/3, 1.03/2, 2.0\}$.

by determining a center, while γ controls the extend of contraction or expansion of the augmented sample around this center. In particular, for a one-hot encoding matrix \mathbf{A} , $\Pi_{\mathbf{A}}^{(i)}\mathbf{X}$ defines the centroid of the cluster to which sample i belongs. Then, the modified samples are located on the ray that originates from the centroid and goes through the original data point $(\mathbf{X}^{(i)}, \mathbf{Y}^{(i)})$. As γ increases, the augmented samples move towards their corresponding centroid and specifically, for $\gamma = 1$ they coincide with the original samples. Furthermore, the cluster size, regulated by the number of clusters q , directly impacts the number of samples mixed together; with smaller clusters, fewer samples are combined. Applying ADA on each minibatch introduces further diversity and enhances robustness, because the composition of samples being mixed together and the value of γ changes in each minibatch. In Appendix A.2 we provide a detailed explanation and analysis of the impact of ADA hyperparameters, q controlling the number of clusters and α controlling the range of values for γ . In Appendix B.4 we empirically show how regression performance varies with respect to these hyperparameters.

In Figure 1, we visually illustrate the augmentation effects of ADA. We uniformly sampled 30 data points between ± 3 (i.e. $x_i \sim \mathcal{U}[-3, 3]$) and set the corresponding target variable as $y_i = \cos(\pi x_i)$ without added noise. We then clustered this data in $q = 5$ and $q = 12$ groups using k-means and applied eq. (7) and eq. (8) to the 30 samples with $\gamma \in \{1/2, 2/3, 1, 3/2, 2\}$ resulting in 150 augmented data points.

3.1 Comparison to C-Mixup

ADA can be interpreted as a generalized variant of C-Mixup [49]. In C-Mixup samples are mixed in pairs, and the combination probability of each sample pair is given by the similarity of their labels, measured by a Gaussian kernel. Augmented samples are then obtained as the convex combination between the pair. In contrast, ADA allows mixing multiple samples based on their cluster membership and the resulting augmentations that may reside in the convex hull of the original samples of a cluster if $\gamma \geq 1$ or beyond it when $\gamma < 1$. In particular, ADA and C-Mixup augmentations would be similar if the anchor matrix \mathbf{A} indicates pairs of samples weighted by the similarity of their labels and $\gamma > 1$.

3.2 Preserving nonlinear data structure

In the following we show that the scaled transformations in eq. (5) and eq. (6) preserve the nonlinear relationship, so that we can use the modified pair $(\tilde{\mathbf{X}}_{\gamma, \mathbf{A}}, \tilde{\mathbf{Y}}_{\gamma, \mathbf{A}})$ to augment the dataset (\mathbf{X}, \mathbf{Y}) . Let $(\mathbf{X}^{(i)}, \mathbf{Y}^{(i)})$ be the i th sample from P_{train} corresponding to the i th row of \mathbf{X} and i th component of \mathbf{Y} . When the data has a nonlinear relation,

$$\mathbf{Y}^{(i)} = f_b(\mathbf{X}^{(i)}) + \epsilon^{(i)} \quad (9)$$

given the zero mean noise variable $\epsilon^{(i)}$, we can alter the anchor loss accordingly [4],

$$b_{\text{NONLIN}, \gamma, \mathbf{A}, f_{\gamma, \mathbf{A}}} = \arg \min_{b, f} \mathbb{E}_{P_{\text{train}}} [((\text{Id} - \mathbf{P}_A)(y - f_b(X)))^2] + \gamma \mathbb{E}_{P_{\text{train}}} [(\mathbf{P}_A(y - f_b(X)))^2],$$

The AR modification Equations 5 and 6 do not preserve the nonlinear relation between the target and predictors,

$$\tilde{\mathbf{Y}}^{(i)} \neq f_b(\tilde{\mathbf{X}}^{(i)}) + \tilde{\epsilon}^{(i)}$$

with another zero mean variable $\tilde{\epsilon}^{(i)}$ operating as the observation noise in the augmented data. Therefore, we propose to further extend the original AR and perform the data augmentation with

scaled transformations to get the modified sample $(\tilde{\mathbf{X}}_{\gamma, \mathbf{A}}^{(i)}, \tilde{\mathbf{Y}}_{\gamma, \mathbf{A}}^{(i)})$ which approximately preserves the nonlinear relationship of sample $(\mathbf{X}^{(i)}, \mathbf{Y}^{(i)})$ as shown below.

We can rewrite $\tilde{\mathbf{Y}}_{\gamma, \mathbf{A}}^{(i)}$ in Equation (8) as

$$\tilde{\mathbf{Y}}_{\gamma, \mathbf{A}}^{(i)} = \frac{f_b(\mathbf{X}^{(i)}) + (\sqrt{\gamma} - 1)(\mathbf{\Pi}_{\mathbf{A}})^{(i)} \mathbf{F}_b(\mathbf{X})}{1 + (\sqrt{\gamma} - 1) \sum_j (\mathbf{\Pi}_{\mathbf{A}})^{(ij)}} + \tilde{\epsilon}_{\gamma, \mathbf{A}}^{(i)}$$

where $\tilde{\epsilon}_{\gamma, \mathbf{A}}^{(i)}$ is a zero mean noise variable and $\mathbf{F}_b(\mathbf{X}) = [f_b(\mathbf{X}^{(1)}), \dots, f_b(\mathbf{X}^{(n)})]^T$. In Appendix A.1, for continuously differentiable function f , we can use the first order Taylor expansion of $\tilde{\mathbf{Y}}_{\gamma, \mathbf{A}}^{(i)}$ around $\tilde{\mathbf{X}}_{\gamma, \mathbf{A}}^{(i)}$ to show that

$$\tilde{\mathbf{Y}}_{\gamma, \mathbf{A}}^{(i)} \approx f_b(\tilde{\mathbf{X}}_{\gamma, \mathbf{A}}^{(i)}) + \tilde{\epsilon}_{\gamma, \mathbf{A}}^{(i)} \quad (10)$$

which approximately has the same nonlinear relation as the original model for small $\|\mathbf{X}^{(i)} - \tilde{\mathbf{X}}_{\gamma, \mathbf{A}}^{(i)}\|_2$ or $\|\sum_j (\mathbf{\Pi}_{\mathbf{A}})^{(ij)} (\mathbf{X}^{(j)} - \tilde{\mathbf{X}}_{\gamma, \mathbf{A}}^{(i)})\|_2$.

With the one-hot partitioning matrix, \mathbf{A} (introduced in the previous section), the approximation of the true nonlinear model becomes accurate in partitions with small diameter (where we define partition diameter as the maximum distance of two samples $\mathbf{X}^{(i)}$ and $\mathbf{X}^{(j)}$ in the same cluster).

3.3 Algorithm

Finally, in this section, we present the ADA algorithm step by step (Algorithm 1) to generate minibatches of data that can be used to train neural networks (or any other nonlinear regressor) by any stochastic gradient descent method. As discussed previously, we propose to repeat the augmentation with different parameter combinations for each minibatch.

Given a centered training dataset (\mathbf{X}, \mathbf{Y}) , its clustering assignment \mathbf{A} , and prior function $p(\gamma)$, the ADA minibatch algorithms takes L random samples from the training set and its corresponding rows in \mathbf{A} and outputs an L -sample mini-bath $(\tilde{\mathbf{X}}_{\gamma, \mathbf{A}}, \tilde{\mathbf{Y}}_{\gamma, \mathbf{A}})$.

In order to do so, we first choose γ according to the provided criterion $p(\gamma)$ (line 3). The corresponding projection matrix $\mathbf{\Pi}_{\mathbf{A}}$ is computed from \mathbf{A} (line 4). Finally, in lines five to seven, the transformation is applied according to Equations 7 and 8.

4 Experiments

We experimentally investigate and compare the performance of ADA. First, we use ADA in an in-distribution setting for a linear regression problem (Section 4.1), in which we show that even in this case, ADA provides improved performance in the low data regime. Second, in Section 4.2, we apply ADA and C-Mixup to the California and Boston Housing datasets as we increase the number of training samples. In the last two subsections, we replicate the in-distribution generalization (Section 4.3) and the out-of-distribution Robustness (Section 4.4) from the C-Mixup paper [49]. In [49] the authors further assess a task generalization experiment. However, the corresponding code was not publicly provided, and a comparison could not be easily made.

Algorithm 1 ADA: Minibatch generation

- 1: **Input:** L training data points (\mathbf{X}, \mathbf{Y}) ;
prior distribution for γ : $p(\gamma)$
 $L \times q$ binary matrix \mathbf{A} with a one per row
indicating the clustering assignment for each
sample.
 - 2: **Output:** $(\tilde{\mathbf{X}}, \tilde{\mathbf{Y}})$
 - 3: Sample γ from $p(\gamma)$
 - 4: Projection matrix: $\mathbf{\Pi}_{\mathbf{A}} \leftarrow \mathbf{A}(\mathbf{A}^T \mathbf{A})^\dagger \mathbf{A}^T$
 - 5: **for** $i = 0$ **to** row of \mathbf{X} **do**
 - 6: $\tilde{\mathbf{X}}_{\gamma, \mathbf{A}}^{(i)} \leftarrow \frac{\mathbf{X}^{(i)} + (\sqrt{\gamma} - 1)(\mathbf{\Pi}_{\mathbf{A}})^{(i)} \mathbf{X}}{1 + (\sqrt{\gamma} - 1) \sum_j (\mathbf{\Pi}_{\mathbf{A}})^{(ij)}}$
 - 7: $\tilde{\mathbf{Y}}_{\gamma, \mathbf{A}}^{(i)} \leftarrow \frac{\mathbf{Y}^{(i)} + (\sqrt{\gamma} - 1)(\mathbf{\Pi}_{\mathbf{A}})^{(i)} \mathbf{Y}}{1 + (\sqrt{\gamma} - 1) \sum_j (\mathbf{\Pi}_{\mathbf{A}})^{(ij)}}$
 - 8: **end for**
 - 9: **return** $(\tilde{\mathbf{X}}_{\gamma, \mathbf{A}}, \tilde{\mathbf{Y}}_{\gamma, \mathbf{A}})$
-

4.1 Linear synthetic data

Using synthetic linear data, we investigate if ADA can improve model performance in an over-parameterized setting compared to C-Mixup, vanilla augmentation, or classical expected risk minimization (ERM). Additionally, we analyze the sensitivity of our approach to the choice of γ and the number of augmentations.

Data: The generated data follows a standard linear structure

$$\mathbf{Y}^{(i)} = \left(\mathbf{X}^{(i)}\right)^T b + b_0 + \epsilon^{(i)} \tag{11}$$

with $\mathbf{X}^{(i)}, b \in \mathbb{R}^{19}$ and $\mathbf{Y}^{(i)}, b_0, \epsilon^{(i)} \in \mathbb{R}$. The parameters are sampled randomly from a Gaussian distribution $N(0, 1)$. We sample 20 different training datasets and one validation set with $\epsilon \sim \mathcal{N}(0, 0.1^2)$, $\mathbf{X}^{(i)} \sim \mathcal{N}(\mathbf{0}, \mathbf{I}_{19})$. For each training set, we take subsets with an increasing number of samples to evaluate the methods on different levels of data availability. The subsets are hierarchically constructed (i.e., meaning a smaller set is always a subset of a larger one). The validation set has 100,000 samples.

Models and Comparisons: We investigate and compare the impact of ADA using two different models with varying complexity: a linear Ridge regression and a multilayer perceptron (MLP) with one hidden layer and 10 units with ReLU activation. Using an MLP with more hidden layers shows similar results (see Appendix B.1 for details).

The ERM models only use the original data. We perform vanilla data augmentation by adding Gaussian noise $\epsilon' \sim N(0, 0.1^2)$ to the output leaving the input unchanged. Next, we apply C-Mixup with a bandwidth of 1 and set the α of the Beta-distribution to 2. Finally, we apply ADA with varying the number of obtained augmentations $k = \{10, 100\}$ and varying range of values for γ . To be precise, we define $\alpha \in \{2, 4, 6, 8, 10\}$ and specify $\beta_i = 1 + \frac{\alpha-1}{k/2} \cdot i$ (with $i \in \{1, \dots, k/2\}$) and $\gamma \in \{\frac{1}{\alpha}, \frac{1}{\beta_{k/2-1}}, \dots, \frac{1}{\beta_1}, 1, \beta_1, \dots, \beta_{k/2-1}, \alpha\}$. \mathbf{A} is constructed using k-means clustering with $q = 8$.

For the Ridge regression model, we increase the dataset by a factor of 10 by sampling from the respective augmentation methods and subsequently compute the regression estimators. In contrast, for the MLP, we implement the augmentation methods on a minibatch level. Specifically, we incorporate vanilla augmentation by adding Gaussian noise to each batch, apply C-Mixup after sampling from the beta distribution in each batch, and finally, apply ADA after sampling from the defined gamma values in each batch.

Results: We plot our results in Figure 2. First, as expected, Ridge regression outperforms the MLP model. Second, when there is little data availability, using ADA decreases the test error compared to ERM. The effect diminishes when the training dataset is sufficiently large, and all models converge to the noise limit of 0.1^2 . Third, vanilla augmentation achieves similar results as ADA and C-Mixup for Ridge regression but not quite for the MLP. This suggests that ADA (and C-Mixup) are more meaningful than randomly adding noise and especially well suited for highly parameterized models as the MLP has almost 20 times more parameters than Ridge regression. In real-world applications, the value of ϵ is usually unknown, and choosing ϵ' for vanilla augmentation is not trivial, especially when the number of samples is small. Fourth, we conclude that generating more augmentations (100 instead of 10) further improves prediction error in vanilla and anchor augmentation (Appendix B Figure 9) and the effectiveness of anchor augmentation is further increased as the range for γ is wider (Appendix B Figure 10). Finally, C-Mixup and ADA perform similarly with ADA having a tendency to achieve a lower test error.

In summary, even in the simplest of cases, in which we should not expect gains from ADA (or C-Mixup), these data augmentation strategies provide gains in performance when the number of training examples is not sufficient to achieve the error floor.

4.2 Housing nonlinear regression

We extend the results from the previous section to the California and Boston housing data and compare ADA to C-Mixup [49]. We repeat the same experiments on three different regression datasets. Results are provided in Appendix B.2 and also show the superiority of ADA over C-Mixup for data augmentation in the implemented experimental setup.

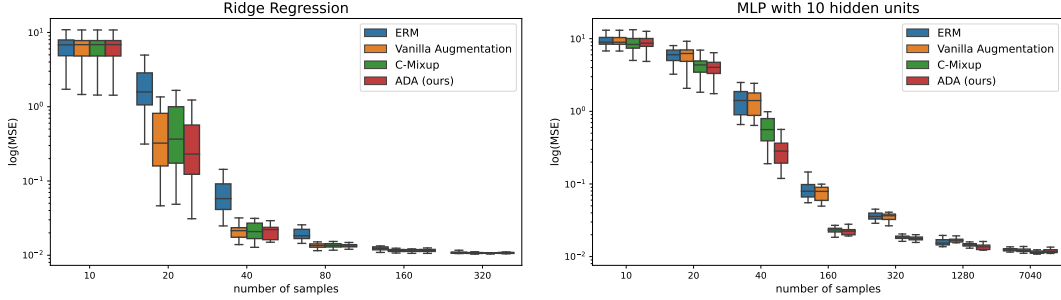


Figure 2: Mean Squared Error for Ridge Regression model and MLP model with varying number of training samples. For Ridge regression, vanilla augmentation and C-Mixup generate $k = 10$ augmented observations per observations. Similarly, Anchor Augmentation generates $k = 10$ augmented observations per observation with parameter $\alpha = 10$.

Data: We use the California housing dataset [19] and the Boston housing dataset [14]. The training dataset contains up to $n = 406$ samples, and the remaining samples are for validation. We report the results as a function of the number of training points.

Models and comparisons: We fit a ridge regression model (baseline) and train a MLP with one hidden layer with a varying number of hidden units with sigmoid activation. The baseline models only use only the original data. We train the same models using C-Mixup with a Gaussian kernel and bandwidth of 1.75. We compare the previous approaches to models fitted on ADA augmented data. We generate 20 different augmentations per original observation using different values for γ controlled via $\alpha = 4$ similar to what was described in Section 4.1. The Anchor matrix is constructed using k-means clustering with $q = 10$.

Results: We report the results in Figure 3. First, we observe that the MLPs outperform Ridge regression suggesting a nonlinear data structure. Second, when the number of training samples is low, applying ADA improves the performance of all models compared to C-Mixup and the baseline. The performance gap decreases as the number of samples increases. When comparing C-Mixup and ADA, we see that using sufficiently many samples both methods achieve similar performance. While on the Boston data, the performance gap between the baseline and ADA persists, on California housing, the non-augmented model fit performs better than the augmented one when data availability increases. This suggests that there is a sweet spot where the addition of original data samples is required for better generalization, and augmented samples cannot contribute any further.

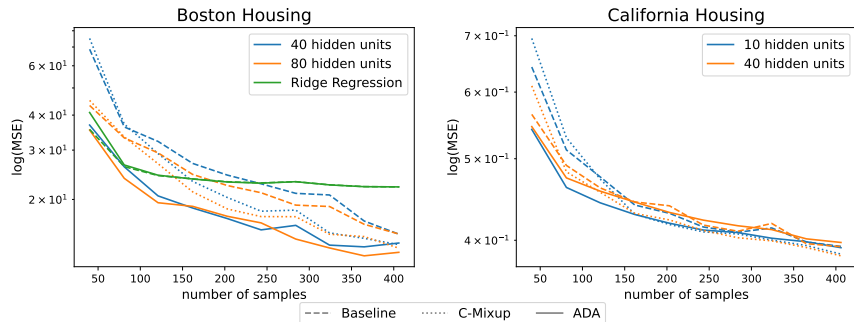


Figure 3: MSE for housing datasets averaged over 10 different train-validation-test splits. On California housing Ridge regression performs much worse which is why it is not considered further (see Appendix B.2).

4.3 In-distribution Generalization

In this section, we evaluate the performance of ADA and compare it to prior approaches on tasks involving in-distribution generalization. We use the same datasets as [49] and closely follow their experimental setup.

Data: We use four of the five in-distribution datasets used in [49]. The validation and test data are expected to follow the same distribution as the training data. Airfoil Self-Noise (Airfoil) and NO2 [24] are both tabular datasets, whereas Exchange-Rate and Electricity [27] are time series datasets. We divide the datasets into train-, validation- and test data randomly, as the authors of C-Mixup did. For Echocardiogram videos [37] (the 5th dataset in [49]), we could not replicate their preprocessing.

Models and comparisons: We compare our approach, ADA, to C-Mixup [49], Local-Mixup [2], Manifold-Mixup [46], Mixup [51] and classical expected risk minimization (ERM). Following the work of [49], we use the same model architectures: a three-layer fully connected network for the tabular datasets; and an LST-Attn [27] for the time series.

We follow the setup of [49] and apply C-Mixup, Manifold-Mixup, Mixup, and ERM with their reported hyperparameters and provided code. For the ADA and Local-Mixup experiments, we use hyperparameter tuning and grid search to find the optimal training (batch size, learning rate, and number of epochs), and Local-Mixup parameters (distance threshold ϵ) and ADA parameters (number of clusters, range of γ , and whether to use manifold augmentation). We provide a detailed description in Appendix B.4. The evaluation metrics are Root Mean Squared Error (RMSE) and Mean Averaged Percentage Error (MAPE).

Results: We report the results in Table 1. For full transparency, in the last row, we copy the results from [49]. We can assess that ADA is competitive with C-Mixup and superior to the other data augmentation strategies. ADA consistently improves the regression fit compared to ERM. Under the same conditions (split of data and Neural network structure), ADA is superior to C-Mixup. But, the degree of improvement is marginal on some datasets and as we show in the last row, we could not fully replicate their results. The only data in which ADA is significantly better than C-Mixup and the other strategies is for the Airfoil data, in which ADA reduces the error by around 15% with respect to the ERM solution.

Table 1: Results for in-distribution generalization. We report the average RMSE and MAPE of three different seeds. Standard deviations are reported in Appendix B.4. The best results per column are printed in bold and the second-best results are underlined (not applicable to the last row).

	Airfoil		NO2		Exchange-Rate		Electricity	
	RMSE	MAPE	RMSE	MAPE	RMSE	MAPE	RMSE	MAPE
ERM	<u>2.758</u>	1.694	0.529	13.402	0.024	2.437	0.058	13.915
Mixup	3.264	1.964	0.522	13.226	0.025	2.513	<u>0.058</u>	13.839
ManiMixup	3.092	1.871	0.528	13.358	0.025	2.541	0.058	14.031
Local Mixup	3.373	2.043	0.524	13.309	<u>0.021</u>	<u>2.136</u>	0.063	14.238
C-Mixup	2.800	<u>1.629</u>	<u>0.516</u>	13.069	0.024	2.431	0.057	<u>13.512</u>
ADA	2.360	1.373	0.515	<u>13.128</u>	0.021	2.116	0.059	13.464
C-Mixup in [49]	2.717	1.610	0.509	12.998	0.020	2.041	0.057	13.372

4.4 Out-of-distribution Robustness

In this section, we evaluate the performance of ADA and compare it to prior approaches on tasks involving out-of-distribution robustness. We use the same datasets as [49] and closely follow their experimental setup.

Data: We use four of the five out-of-distribution datasets used in [49]. First, we use RCFashion-MNIST (RCF-MNIST) [49], which is a synthetic modification of Fashion-MNIST that models subpopulation shifts. Second, we investigate domain shifts using Communities and Crime (Crime) [12], SkillCraft1 Master Table (SkillCraft) [12] and Drug-target Interactions (DTI) [17] all of which are tabular datasets. For Crime, we use state identification, in SkillCraft we use "League Index", which corresponds to different levels of competitors, and in DTI we use year, as domain information. We split the datasets into train-, validation- and test data based on the domain information resulting in domain-distinct datasets. We provide a detailed description of datasets in Appendix B.4. Due to computational complexity, we could not establish a fair comparison on the satellite image regression dataset [23] (the fifth dataset in [49]), so we report some exploratory results in Appendix B.4.

Models and comparisons: As detailed in Section 4.3. Additionally, we use a ResNet-18 [15] for RCF-MNIST and DeepDTA [38] for DTI, as proposed in [49].

Results: We report the RMSE and the "worst" domain RMSE, which corresponds to the worst within-domain RMSE for out-of-domain test sets in Table 2. Similar to [49], we report the R value for the DTI dataset (higher values suggest a better fit of the regression model). For full transparency, in the last row, we copy the results from [49]. We can assess that ADA is competitive with C-Mixup and the other data augmentation strategies. Under the same conditions (split of data and Neural network structure), ADA is superior to C-Mixup. But, the degree of improvement is marginal on some datasets and as we show in the last row, we could not fully replicate their results. ADA is significantly better than C-Mixup and other strategies on the SkillCraft data, in which ADA reduces the error by around 15% compared to the ERM solution.

Table 2: Results for out-of-distribution generalisation. We report the average RMSE across domains in the test data and the "worst within-domain RMSE over three different seeds. For the DTI dataset, we report average R and "worst within-domain" R. Standard deviations are reported in Appendix B.4. The best results per column are printed in bold and the second-best results are underlined (not applicable to the last row).

	RCF-MNIST	Crimes		SkillCraft		DTI	
	avg. RMSE	avg. RMSE	worst RMSE	avg. RMSE	worst RMSE	avg. R	worst R
ERM	0.164	0.136	0.170	6.147	<u>7.906</u>	<u>0.483</u>	<u>0.439</u>
Mixup	0.159	0.134	0.168	6.460	9.834	0.459	0.424
ManiMixup	0.157	0.128	0.155	<u>5.908</u>	9.264	0.474	0.431
LocalMixup	0.187	0.133	0.1590	7.251	10.996	0.470	0.433
C-Mixup	<u>0.158</u>	0.132	0.165	6.216	8.223	0.474	0.435
ADA	0.175	<u>0.130</u>	<u>0.156</u>	5.301	6.877	0.493	0.448
C-Mixup in [49]	0.146	0.123	0.146	5.201	7.362	0.498	0.458

5 Conclusion

We introduced Anchor Data Augmentation (ADA), an extension of Anchor Regression for the purpose of data augmentation. AR is a novel causal approach to increase the robustness in regression problems. In ADA, we systematically mix multiple samples based on a collective similarity criterion, which is determined via clustering. The augmented samples are modifications of the original samples that are moved towards or away from the cluster centroids based on the desired degree of robustness in AR. Our empirical evaluations across diverse synthetic and real-world regression problems consistently demonstrate the effectiveness of ADA, especially for limited data availability. ADA is competitive with or outperforms state-of-the-art data augmentation strategies for regression problems, even though the improvements are marginal on some datasets.

ADA can be applied to any regression setting, and we have not found any case in which the results were detrimental. To apply ADA, we only need to cluster our data and select a distribution for γ . We relied on vanilla *k-means*, and the results are robust with respect to the number of clusters. Other clustering algorithms might be more suitable for different applications. For setting the parameter γ , we used a uniform distribution. We believe a gamma distribution could be equally effective.

Broader Impact

The purpose of data augmentation is to compensate for data scarcity in multiple domains where gathering and labeling data accurately by experts is impractical, expensive, or time-consuming. If applied properly, it can effectively expand the training dataset, reduce overfitting and improve the model's robustness, as was shown in the paper. However, It is important to note that the choice and combination of the data augmentation technique depends on the specific problem and using the wrong augmentation method may introduce additional bias to the model. More generally, incorrect data augmentation can lead to the following problems: overfitting the augmented data, loss of important information, introduction of unrealistic patterns and imbalanced presentation of the data. Detecting emerging problems due to data augmentation may not be straightforward. In particular, the performance on a test distribution that matches the training data distribution may be misleading and the model's predictions should be used with caution on new data that reflects the potential distribution shifts or variations encountered in real-world.

References

- [1] Antreas Antoniou, Amos Storkey, and Harrison Edwards. Data augmentation generative adversarial networks. *arXiv preprint arXiv:1711.04340*, 2017.
- [2] Raphael Baena, Lucas Drumetz, and Vincent Gripon. Preventing manifold intrusion with locality: Local mixup. *arXiv preprint arXiv:2201.04368*, 2022.
- [3] Xavier Bouthillier, Kishore Konda, Pascal Vincent, and Roland Memisevic. Dropout as data augmentation. *arXiv preprint arXiv:1506.08700*, 2015.
- [4] Peter Bühlmann. Invariance, causality and robustness. *Statistical Science*, 35(3):404–426, 2020.
- [5] Luigi Carratino, Moustapha Cissé, Rodolphe Jenatton, and Jean-Philippe Vert. On mixup regularization. *The Journal of Machine Learning Research*, 23(1):14632–14662, 2022.
- [6] Clément Chadebec and Stéphanie Allasonnière. Data augmentation with variational autoencoders and manifold sampling. In *Deep Generative Models, and Data Augmentation, Labelling, and Imperfections*, pages 184–192. Springer, 2021.
- [7] Ekin D Cubuk, Barret Zoph, Dandelion Mane, Vijay Vasudevan, and Quoc V Le. Autoaugment: Learning augmentation strategies from data. In *Proceedings of the IEEE/CVF conference on computer vision and pattern recognition workshops*, pages 113–123, 2019.
- [8] Ekin D Cubuk, Barret Zoph, Jonathon Shlens, and Quoc V Le. Randaugment: Practical automated data augmentation with a reduced search space. In *Proceedings of the IEEE/CVF conference on computer vision and pattern recognition workshops*, pages 702–703, 2020.
- [9] Jia Deng, Wei Dong, Richard Socher, Li-Jia Li, Kai Li, and Li Fei-Fei. Imagenet: A large-scale hierarchical image database. In *2009 IEEE conference on computer vision and pattern recognition*, pages 248–255. Ieee, 2009.
- [10] Terrance DeVries and Graham W Taylor. Improved regularization of convolutional neural networks with cutout. *arXiv preprint arXiv:1708.04552*, 2017.
- [11] Vanessa Didelez, Sha Meng, and Nuala A Sheehan. Assumptions of iv methods for observational epidemiology. *Statistical Science*, 25(1):22–40, 2010.
- [12] Dheeru Dua and Casey Graff. UCI machine learning repository, 2017.
- [13] Ian Goodfellow, Jean Pouget-Abadie, Mehdi Mirza, Bing Xu, David Warde-Farley, Sherjil Ozair, Aaron Courville, and Yoshua Bengio. Generative adversarial networks. *Communications of the ACM*, 63(11):139–144, 2020.
- [14] David Harrison and Daniel L Rubinfeld. Hedonic housing prices and the demand for clean air. *Journal of Environmental Economics and Management*, 5(1):81–102, 1978.
- [15] Kaiming He, Xiangyu Zhang, Shaoqing Ren, and Jian Sun. Deep residual learning for image recognition. In *Proceedings of the IEEE conference on computer vision and pattern recognition*, pages 770–778, 2016.
- [16] Daniel Ho, Eric Liang, Xi Chen, Ion Stoica, and Pieter Abbeel. Population based augmentation: Efficient learning of augmentation policy schedules. In *International Conference on Machine Learning*, pages 2731–2741. PMLR, 2019.
- [17] Kexin Huang, Tianfan Fu, Wenhao Gao, Yue Zhao, Yusuf Roohani, Jure Leskovec, Connor W Coley, Cao Xiao, Jimeng Sun, and Marinka Zitnik. Therapeutics data commons: Machine learning datasets and tasks for drug discovery and development. *arXiv preprint arXiv:2102.09548*, 2021.
- [18] Seong-Hyeon Hwang and Steven Euijong Whang. Regmix: Data mixing augmentation for regression. *arXiv preprint arXiv:2106.03374*, 2021.
- [19] R. Kelley Pace and Ronald Barry. Sparse spatial autoregressions. *Statistics and Probability Letters*, 33(3):291–297, 1997.

- [20] Jang-Hyun Kim, Wonho Choo, Hosan Jeong, and Hyun Oh Song. Co-mixup: Saliency guided joint mixup with supermodular diversity. *arXiv preprint arXiv:2102.03065*, 2021.
- [21] Jang-Hyun Kim, Wonho Choo, and Hyun Oh Song. Puzzle mix: Exploiting saliency and local statistics for optimal mixup. In *International Conference on Machine Learning*, pages 5275–5285. PMLR, 2020.
- [22] Diederik P Kingma and Max Welling. Auto-encoding variational bayes. *arXiv preprint arXiv:1312.6114*, 2013.
- [23] Pang Wei Koh, Shiori Sagawa, Henrik Marklund, Sang Michael Xie, Marvin Zhang, Akshay Balsubramani, Weihua Hu, Michihiro Yasunaga, Richard Lanus Phillips, Irena Gao, et al. Wilds: A benchmark of in-the-wild distribution shifts. In *International Conference on Machine Learning*, pages 5637–5664. PMLR, 2021.
- [24] Charles Kooperberg. Statlib: an archive for statistical software, datasets, and information. *The American Statistician*, 51(1):98, 1997.
- [25] Alex Krizhevsky, Geoffrey Hinton, et al. Learning multiple layers of features from tiny images. 2009.
- [26] Alex Krizhevsky, Ilya Sutskever, and Geoffrey E Hinton. Imagenet classification with deep convolutional neural networks. *Advances in neural information processing systems*, 25, 2012.
- [27] Guokun Lai, Wei-Cheng Chang, Yiming Yang, and Hanxiao Liu. Modeling long-and short-term temporal patterns with deep neural networks. In *The 41st international ACM SIGIR conference on research & development in information retrieval*, pages 95–104, 2018.
- [28] Balaji Lakshminarayanan, Alexander Pritzel, and Charles Blundell. Simple and scalable predictive uncertainty estimation using deep ensembles. *Advances in neural information processing systems*, 30, 2017.
- [29] Yann LeCun, Léon Bottou, Yoshua Bengio, and Patrick Haffner. Gradient-based learning applied to document recognition. *Proceedings of the IEEE*, 86(11):2278–2324, 1998.
- [30] Sungbin Lim, Ildoo Kim, Taesup Kim, Chiheon Kim, and Sungwoong Kim. Fast autoaugment. *Advances in Neural Information Processing Systems*, 32, 2019.
- [31] Chen Lin, Minghao Guo, Chuming Li, Xin Yuan, Wei Wu, Junjie Yan, Dahua Lin, and Wanli Ouyang. Online hyper-parameter learning for auto-augmentation strategy. In *Proceedings of the IEEE/CVF International Conference on Computer Vision*, pages 6579–6588, 2019.
- [32] Tom Ching LingChen, Ava Khonsari, Amirreza Lashkari, Mina Rafi Nazari, Jaspreet Singh Sambee, and Mario A Nascimento. Uniformaugment: A search-free probabilistic data augmentation approach. *arXiv preprint arXiv:2003.14348*, 2020.
- [33] Zicheng Liu, Siyuan Li, Di Wu, Zihan Liu, Zhiyuan Chen, Lirong Wu, and Stan Z Li. Automix: Unveiling the power of mixup for stronger classifiers. In *European Conference on Computer Vision*, pages 441–458. Springer, 2022.
- [34] Zirui Liu, Haifeng Jin, Ting-Hsiang Wang, Kaixiong Zhou, and Xia Hu. Divaug: Plug-in automated data augmentation with explicit diversity maximization. In *Proceedings of the IEEE/CVF International Conference on Computer Vision*, pages 4762–4770, 2021.
- [35] J MacQueen. Classification and analysis of multivariate observations. In *5th Berkeley Symp. Math. Statist. Probability*, pages 281–297, 1967.
- [36] Samuel G Müller and Frank Hutter. Trivialaugment: Tuning-free yet state-of-the-art data augmentation. In *Proceedings of the IEEE/CVF International Conference on Computer Vision*, pages 774–782, 2021.
- [37] David Ouyang, Bryan He, Amirata Ghorbani, Neal Yuan, Joseph Ebinger, Curtis P Langlotz, Paul A Heidenreich, Robert A Harrington, David H Liang, Euan A Ashley, et al. Video-based ai for beat-to-beat assessment of cardiac function. *Nature*, 580(7802):252–256, 2020.

- [38] Hakime Öztürk, Arzucan Özgür, and Elif Ozkirimli. Deepdta: deep drug–target binding affinity prediction. *Bioinformatics*, 34(17):i821–i829, 2018.
- [39] Jonas Peters, Dominik Janzing, and Bernhard Schölkopf, editors. *Elements of Causal Inference*. MIT Press, Cambridge, MA, 2017.
- [40] Jonas Peters, Nicolai Meinshausen, and Peter Bühlmann. Causal inference by using invariant prediction: Identification and confidence intervals. *Journal of the Royal Statistical Society Series B*, 78(5):947–1012, 2016.
- [41] Mateo Rojas-Carulla, Bernhard Schölkopf, Richard Turner, and Jonas Peters. Invariant models for causal transfer learning. *The Journal of Machine Learning Research*, 19(1):1309–1342, 2018.
- [42] Dominik Rothenhäusler, Nicolai Meinshausen, Peter Bühlmann, Jonas Peters, et al. Anchor regression: Heterogeneous data meet causality. *Journal of the Royal Statistical Society Series B*, 83(2):215–246, 2021.
- [43] Karen Simonyan and Andrew Zisserman. Very deep convolutional networks for large-scale image recognition. *arXiv preprint arXiv:1409.1556*, 2014.
- [44] Zhiqiang Tang, Yunhe Gao, Leonid Karlinsky, Prasanna Sattigeri, Rogerio Feris, and Dimitris Metaxas. Onlineaugment: Online data augmentation with less domain knowledge. In *European Conference on Computer Vision*, pages 313–329. Springer, 2020.
- [45] Luke Taylor and Geoff Nitschke. Improving deep learning with generic data augmentation. In *2018 IEEE Symposium Series on Computational Intelligence (SSCI)*, pages 1542–1547. IEEE, 2018.
- [46] Vikas Verma, Alex Lamb, Christopher Beckham, Amir Najafi, Ioannis Mitliagkas, David Lopez-Paz, and Yoshua Bengio. Manifold mixup: Better representations by interpolating hidden states. In *International conference on machine learning*, pages 6438–6447. PMLR, 2019.
- [47] Haotao Wang, Chaowei Xiao, Jean Kossaifi, Zhiding Yu, Anima Anandkumar, and Zhangyang Wang. Augmax: Adversarial composition of random augmentations for robust training. *Advances in neural information processing systems*, 34:237–250, 2021.
- [48] Xiaogang Xu, Hengshuang Zhao, and Philip Torr. Universal adaptive data augmentation. *arXiv preprint arXiv:2207.06658*, 2022.
- [49] Huaxiu Yao, Yiping Wang, Linjun Zhang, James Zou, and Chelsea Finn. C-mixup: Improving generalization in regression. In *Proceeding of the Thirty-Sixth Conference on Neural Information Processing Systems*, 2022.
- [50] Sangdoon Yun, Dongyoon Han, Seong Joon Oh, Sanghyuk Chun, Junsuk Choe, and Youngjoon Yoo. Cutmix: Regularization strategy to train strong classifiers with localizable features. In *Proceedings of the IEEE/CVF international conference on computer vision*, pages 6023–6032, 2019.
- [51] Hongyi Zhang, Moustapha Cisse, Yann N Dauphin, and David Lopez-Paz. mixup: Beyond empirical risk minimization. *arXiv preprint arXiv:1710.09412*, 2017.
- [52] Linjun Zhang, Zhun Deng, Kenji Kawaguchi, Amirata Ghorbani, and James Zou. How does mixup help with robustness and generalization? *arXiv preprint arXiv:2010.04819*, 2020.
- [53] Xinyu Zhang, Qiang Wang, Jian Zhang, and Zhao Zhong. Adversarial autoaugment. *arXiv preprint arXiv:1912.11188*, 2019.

A Additional information for Anchor Data Augmentation

A.1 Derivation of ADA for nonlinear data

In the following, we provide the more detailed derivation to Equation (10), which motivates the usage of the scaled transformation we use in ADA to obtain $(\tilde{\mathbf{X}}_{\gamma, \mathbf{A}}, \tilde{\mathbf{Y}}_{\gamma, \mathbf{A}})$. We use the same notation that was introduced in Section 3. As discussed in Section 3, we can write $\tilde{\mathbf{Y}}_{\gamma, \mathbf{A}}^{(i)}$ in Equation 8 as

(12)

for some noise variable $\tilde{\epsilon}_{\gamma, \mathbf{A}}^{(i)}$, where $\mathbf{F}_b(\mathbf{X}) = [f_b(\mathbf{X}^{(1)}), \dots, f_b(\mathbf{X}^{(n)})]^T$. For differentiable function f with continuous first-order derivative \dot{f} , we can use Taylor expansion around $\tilde{\mathbf{X}}_{\gamma, \mathbf{A}}^{(i)}$ of the nominator and get

$$\begin{aligned} f_b(\mathbf{X}^{(i)}) + (\sqrt{\gamma} - 1)(\Pi_{\mathbf{A}})^{(i)} \mathbf{F}_b(\mathbf{X}) &= f_b(\tilde{\mathbf{X}}_{\gamma, \mathbf{A}}^{(i)}) + (\mathbf{X}^{(i)} - \tilde{\mathbf{X}}_{\gamma, \mathbf{A}}^{(i)})^T \dot{f}_b(\tilde{\mathbf{X}}_{\gamma, \mathbf{A}}^{(i)}) \\ &\quad + (\sqrt{\gamma} - 1) \sum_j (\Pi_{\mathbf{A}})^{(ij)} f_b(\tilde{\mathbf{X}}_{\gamma, \mathbf{A}}^{(i)}) \\ &\quad + (\sqrt{\gamma} - 1) \sum_j (\Pi_{\mathbf{A}})^{(ij)} (\mathbf{X}^{(j)} - \tilde{\mathbf{X}}_{\gamma, \mathbf{A}}^{(i)}) \dot{f}_b(\tilde{\mathbf{X}}_{\gamma, \mathbf{A}}^{(i)}) \\ &\quad + \mathcal{O}(\|\mathbf{X}^{(i)} - \tilde{\mathbf{X}}_{\gamma, \mathbf{A}}^{(i)}\|_2 \|\sum_j (\Pi_{\mathbf{A}})^{(ij)} (\mathbf{X}^{(j)} - \tilde{\mathbf{X}}_{\gamma, \mathbf{A}}^{(i)})\|_2) \\ &= \left(1 + (\sqrt{\gamma} - 1) \sum_j (\Pi_{\mathbf{A}})^{(ij)} \right) f_b(\tilde{\mathbf{X}}_{\gamma, \mathbf{A}}^{(i)}) \\ &\quad + \mathcal{O}(\|\mathbf{X}^{(i)} - \tilde{\mathbf{X}}_{\gamma, \mathbf{A}}^{(i)}\|_2 \|\sum_j (\Pi_{\mathbf{A}})^{(ij)} (\mathbf{X}^{(j)} - \tilde{\mathbf{X}}_{\gamma, \mathbf{A}}^{(i)})\|_2) \end{aligned}$$

where in the second equality we use the fact that coefficient of $\dot{f}_b(\tilde{\mathbf{X}}_{\gamma, \mathbf{A}}^{(i)})$ (in the second and fourth term) is zero for any f_b due the definition of $\tilde{\mathbf{X}}^{(i)}$ in Equation 7 and therefore,

$$\tilde{\mathbf{Y}}_{\gamma, \mathbf{A}}^{(i)} \approx f_b(\tilde{\mathbf{X}}_{\gamma, \mathbf{A}}^{(i)}) + \tilde{\epsilon}_{\gamma, \mathbf{A}}^{(i)}$$

which is approximately similar to the original nonlinear model for small $\|\mathbf{X}^{(i)} - \tilde{\mathbf{X}}_{\gamma, \mathbf{A}}^{(i)}\|_2$ or $\|\sum_j (\Pi_{\mathbf{A}})^{(ij)} (\mathbf{X}^{(j)} - \tilde{\mathbf{X}}_{\gamma, \mathbf{A}}^{(i)})\|_2$.

A.2 Additional information on hyperparameters of ADA

In this section, we illustrate in a simple 1D example (i.e. cosine data used in Figure 1) how changes in the hyperparameter values modify the data and affect the achieved estimation. Additionally, we show in Appendix B.4 how ADA performance on real-world data is impacted by changes in the hyperparameter values.

Having a fixed pair of (γ, \mathbf{A}) enforces the model to learn the optimal parameters for a particular trade-off between performance on P_{train} and predefined interventional distributions [42]. Instead of limiting the regularization to a fixed pair of (γ, \mathbf{A}) that performs well on a previously known set of interventions, we propose to optimize the loss simultaneously over a set of $\gamma \in [0, \infty)$ and different anchor matrices. In particular, we optimize the parameters on a mixture of essentially similar distributions to P_{train} simultaneously. To reduce the anchor regression's regularization effect, we propose using a combination of the following methods to exploit the data invariances and avoid conservative predictions.

Anchor Matrices and Locality: Anchor variable A is assumed to be the exogenous variable that generates heterogeneity in the target and has an approximately linear relation with (X, y) (see AR loss in Equation 3). It is recommended to choose the variable relying on expert knowledge about the features that the target has a higher dependence on or is possibly misrepresented in the dataset so that

we encourage the robustness of the trained model against this type of discrepancy. After deciding the features, one way to construct the anchor matrix \mathbf{A} is to partition the dataset according to the similarity of the features, using for example binning or clustering algorithms. Then we can fill the rows of \mathbf{A} with a one-hot encoding of the partition index that each sample belongs to.

We use the following nonlinear Cosine data model as a running example to demonstrate more clearly how \mathbf{A} is constructed and affects the augmentation procedure.

$$\epsilon \sim \mathcal{N}(0, 0.1^2 \cdot \mathbf{I}), X \sim U(-3\pi, 3\pi), y = \cos(X^T b) + \epsilon, \quad (13)$$

For illustration purposes, we use in Figures 5, 7 equidistant x values as this reduces noise and emphasizes the effect of ADA parameters more.

Further, we note $a : \mathcal{X} \rightarrow \{1, \dots, q\}$ that maps each sample $X \in \mathcal{X}$ to one of q partitions and returns its index. For instance, with an equal width binning scheme one can partition the range of a feature map $g_k : \mathcal{X} \rightarrow [0, B]$ to q parts and set $a(X) := \arg \min_{r \in \{1, \dots, q\}} \{r : r/q \geq g_k(X)\}$. Using, equal size binning scheme, one would first sort $g_k(X^{(i)})$ for $i \in \{1, \dots, n\}$ get the indices $o(g_k(X^{(i)}))$ accordingly and use $a(X^{(i)}) := \arg \min_{r \in \{1, \dots, q\}} \{r : rn/q \geq o(g_k(X))\}$. Similarly, it is possible to use a clustering algorithm such as k-means [35] to partition $\{X^{(i)}\}_i$ into hard clusters based on the similarity of each sample to cluster center $c_r \in \mathcal{X}$ for $r \in \{1, \dots, q\}$ leading to $a(X) := \arg \min_{r \in \{1, \dots, q\}} D(X, c_r)$ for some distance metric $D : \mathcal{X} \times \mathcal{X} \rightarrow [0, \infty)$.

With \mathbf{A} constructed from the one-hot encoding of partition indices of samples, the $\Pi_{\mathbf{A}}$ operator returns the average value of the projected values in the same group as each sample.

$$\begin{aligned} (\Pi_{\mathbf{A}})^{(i)} \mathbf{X} &= \frac{1}{n_r} \sum_{j: a(\mathbf{X}^{(j)})=a(\mathbf{X}^{(i)})} \mathbf{X}^{(j)} \text{ and} \\ (\Pi_{\mathbf{A}})^{(i)} \mathbf{Y} &= \frac{1}{n_r} \sum_{j: a(\mathbf{X}^{(j)})=a(\mathbf{X}^{(i)})} \mathbf{Y}^{(j)}, \end{aligned}$$

where n_r is the size of group with index $r = a(\mathbf{X}^{(i)})$. Getting weighted averages of partition samples is also straightforward by scaling the one-hot encodings of group indices with the squared root of the desired weights.

Partition Size and Number: As was mentioned before, the target should have a high dependence on the anchor variable A . Specifically, with the partitioning scheme explained above, $\tilde{\mathbf{X}}_{\gamma, \mathbf{A}}^{(i)}$ is constructed as a linear combination of $\mathbf{X}^{(i)}$ and the partition average with a target variable constructed in a similar manner. If the generative function f varies significantly in a partition, the average value is going to flatten out the variations and decrease the heterogeneity of the augmented samples in that partition. For a smaller partition size, the augmented data is going to be close to the mean value f and improve the optimization, however, partitions with a smaller number of samples will have a noisier estimation of the sample mean in each partition and deem the augmentation ineffective. We show the same effect of q on the Cosine data model in Figure 4 for γ set via $\alpha = 2$ (as described in Section 4.1) and a different number of groups when $g_k(X) = X$ and K-Means is used for partitioning the dataset. In the groups where f is approximately linear, the augmentation line is approximately tangent to f , specifically when the clusters are small and the cluster average lies close to $\cos(X)$.

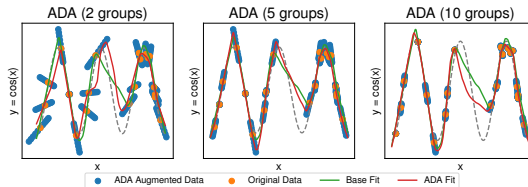


Figure 4: Model predictions for models fit on the original data and ADA augmented data with varying partition sizes. On a hold-out validation set the base model has $MSE = 0.097$. The augmented model achieves MSEs of 0.124, 0.069, 0.079, respectively. We use MLPs with architecture [50, 50, 50, 50, 50] and ReLU activation function. The original data has $n = 20$ points. We use k-means clustering, $\alpha = 2$, and augmented 10 additional points per given point.

Values of γ : For $\gamma \in [0, \infty)$, the transformations in Equation 7 and 8 defines a line passing through $(\mathbf{X}^{(i)}, \mathbf{Y}^{(i)})$ and the group average $((\Pi_{\mathbf{A}})^{(i)}\mathbf{X}, (\Pi_{\mathbf{A}})^{(i)}\mathbf{Y})$. As $|\gamma - 1|$ grows the augmented sample gets further away from $\mathbf{X}^{(i)}$ and in large groups this may result in misleading augmentation. Therefore, when group diameter is large it is important to keep γ close to one. In Figure 5 we show how varying γ changes the efficacy of the augmented samples for the Cosine data model with $q = 2$ groups. To be precise, we vary the range of γ by defining a parameter $\alpha \in \{1.5, 2, 5, 10\}$. We further specify $\beta_i = 1 + \frac{\alpha-1}{k/2} \cdot i$ (with $i \in \{1, \dots, k/2\}$) where k is the number of augmentations and finally $\gamma \in \left\{ \frac{1}{\alpha}, \frac{1}{\beta_{k/2-1}}, \dots, \frac{1}{\beta_1}, 1, \beta_1, \dots, \beta_{k/2-1}, \alpha \right\}$. Additionally, we provide a baseline and an augmented model fit in Figure 6 with different values for γ .

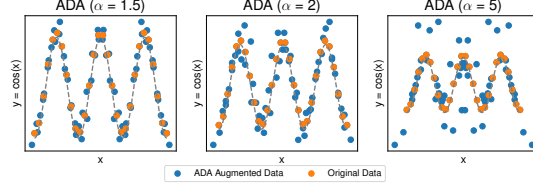


Figure 5: ADA Augmented samples for varying ranges of γ controlled via the parameter α . We use k-means clustering into $q = 5$ groups and augmented 2 additional points per given point.

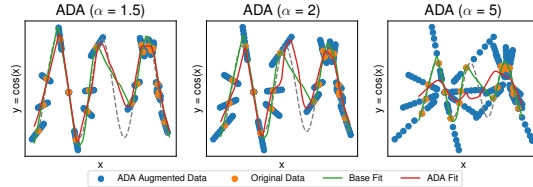


Figure 6: Model predictions for models fit on the original data and ADA augmented data with different ranges of γ controlled via the parameter α . On a hold-out validation set the base model has $MSE = 0.097$. The augmented model fits achieve MSEs of 0.083, 0.124, 0.470, respectively. We use MLPs with architecture [50, 50, 50, 50, 50] and ReLU activation function. The original data has $n = 20$ points. We use k-means clustering into $q = 2$ groups and augmented 10 additional points per given point.

Number of augmentations: For each anchor matrix \mathbf{A} and γ we can add n new samples to the dataset. The addition of more augmented samples may not be beneficial as the optimization may overfit the approximations in the augmented data model in Equation 10. In the Cosine data model this is specifically problematic when X is close to multiples of π as depicted in Figure 7. Additionally, we provide a baseline and an augmented model fit in Figure 8 with different number of augmentations.

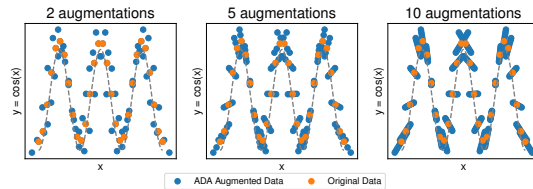


Figure 7: ADA Augmented samples for varying numbers of parameter combinations. We use k-means clustering into $q = 2$ groups $\alpha = 1.5$.

As it is standard practice to use stochastic gradient descent methods for optimizing a regressor, we suggest applying ADA on each minibatch instead of the entire dataset. This avoids choosing a fixed numbers of augmentations. Furthermore, it adds diversity to the "mixing" behavior of ADA, because the samples that are being mixed change in each iteration.

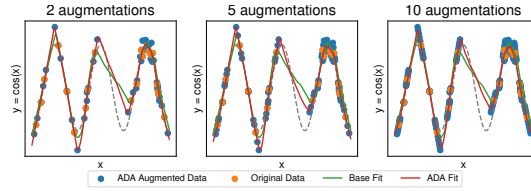


Figure 8: Model predictions for models fit on the original data and ADA augmented data with a different number of parameter combinations (equal number of augmentations). On a hold-out validation set the base model has $MSE = 0.097$. The augmented model fits achieve MSEs of 0.470, 0.071, 0.057, respectively. We use MLPs with architecture $[50, 50, 50, 50, 50]$ and ReLU activation function. The original data has $n = 20$ points. We use k-means clustering into $q = 5$ groups and $\alpha = 2$.

B Experiments

B.1 Linear synthetic data

In this section, we present more detailed results of the experiments on synthetic linear data (Section 4.1). First, Figure 9 shows a comparison of using 10 instead of 100 additional augmentations per original sample using Ridge regression model. Performance increases when using 100 instead of 10 augmentations for all methods, as the resulting prediction error is lower.

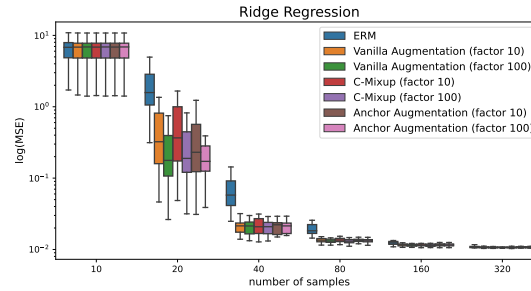


Figure 9: Comparison of augmenting the synthetic linear dataset by a factor of 10 and 100. More augmentations achieve lower MSE on all methods. Here, anchor augmentation is performed for $\alpha = 8$.

Second, we report experimental results for using a wider interval for γ values in Figure 10. The width is controlled via the parameter α , as described in Section 3. While for ridge regression, the effectiveness of anchor augmentation is not sensitive to the choice of α , the MLP model shows more sensitivity.

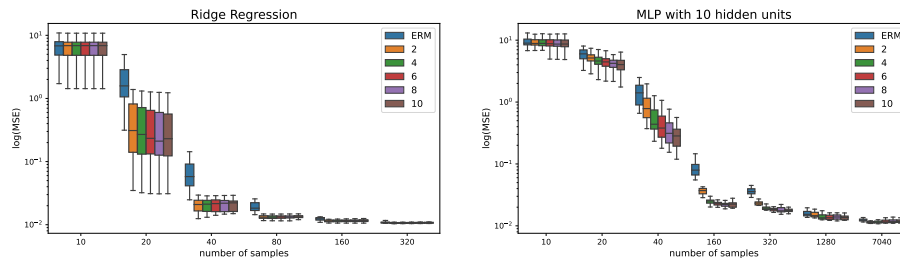


Figure 10: Comparison of augmenting the synthetic linear dataset with different intervals of γ controlled via α . The ridge regression is not sensitive to the choice of α , as different values result in a similar prediction error. Contrary, for the MLP a larger value of α is more effective.

Finally, we report results for using an MLP with 40 hidden units in Figure 11. The results are consistent with the results from the MLP with 10 hidden unity.

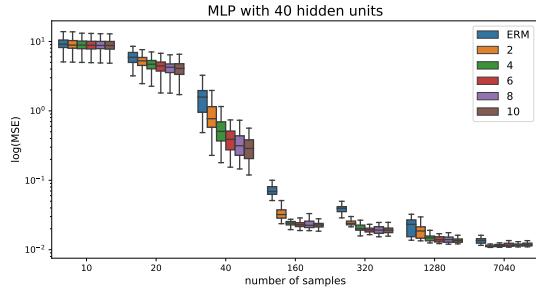


Figure 11: Analysis of the sensitivity of ADA to the choice of α using an MLP with 40 hidden units.

B.2 Additional results for real-world regression data

In Figure 12 we provide additional results showing, that the Ridge regression model performs worse on the California housing data. The experimental setting is the same as described in Section 4.2.

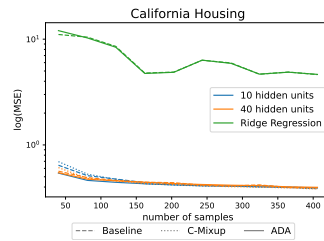


Figure 12: MSE for California housing averaged over 10 different train-validation-test splits.

B.3 Additional results on real-world data

In this section, we provide further experimental results on real-world regression problems. We use the following datasets from the UCI ML repository [12]: *Auto MPG* (7 predictors), *Concrete Compressive Strength* (8 predictors), and *Yacht Hydrodynamics* (6 predictors). The experimental setting follows the one described in Section 4.2, except that we use here to training, validation, and test datasets of relative sizes 50%, 25%, and 25% respectively. We use MLPs with one layer and varying layer width and sigmoid activation. The models are trained using Adam optimization. We generate 9 different dataset splits and report the average prediction error in Figure 13. Similar to the results in Section 4.2, ADA outperforms the baseline and C-Mixup especially when little data is available. The performance gap vanishes when more samples are available demonstrating the effectiveness of ADA in over-parameterized scenarios.

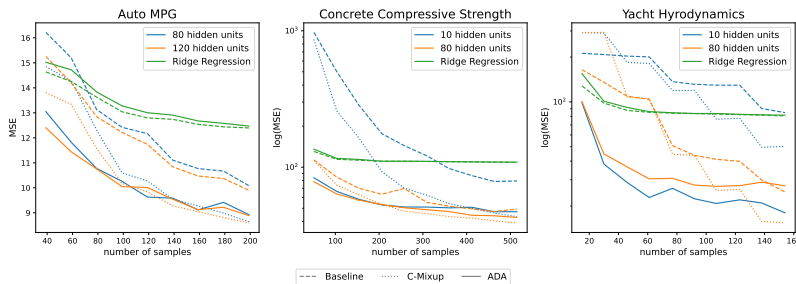


Figure 13: MSE for housing datasets averaged over 9 different train-validation-test splits.

B.4 Details: In-distribution Generalization and Out-of-distribution Robustness

In this section we present details for the experiments described in section 4.3 and Section 4.4. We closely follow the experimental setup of [49].

Data Description

In the following, we provide a more detailed description of the datasets used for in-distribution generalization and out-of-distribution robustness experiments.

Airfoil [12]: is a tabular dataset originating from aerodynamic and acoustic tests of two and three-dimensional airfoil blade sections. Each input has 5 features measuring frequency, angle of attack, chord length, free-stream velocity and suction side displacement thickness. The target variable is the scaled sound pressure level. As in [49], we additionally apply Min-Max normalization on the input features and split the dataset into train (1003 samples), validation (300 samples) and test (200 samples) data.

NO2: is a tabular dataset originating from a study where air pollution at a road is related to traffic volume and meteorological variables. Each input has 7 features measuring, the logarithm of the number of cars per hour, temperature 2 meter above ground, wind speed, the temperature difference between 25 and 2 meters above ground, wind direction, hour of day and day number from 1st October 1 2001. The target variable is the logarithm of the concentration of NO2 particles, measured at Alnabru in Oslo, Norway. Following [49], we split the dataset into a train (200 samples), validation (200 samples) and test data (100 samples).

Exchange-Rate [27]: is a timeseries measuring the daily exchange rate of eight foreign countries including Australia, British, Canada, Switzerland, China, Japan, New Zealand and Singapore ranging from 1990 to 2016. The slide window size is 168 days, therefore the input has dimension 168×8 and the label has dimension 1×8 . Following [27, 49] the dataset is split into training (4,373 samples), validation (1,518 samples) and test data (1,518 samples) in chronological order.

Electricity [27]: is a timeseries measuring the electricity consumption of 321 clients from 2012 to 2014. Similar to [27, 49] we converted the data to reflect hourly consumption. The slide window size is 168 hours, therefore the input has dimension 168×321 and the label has dimension 1×321 . The dataset is split into training (15,591 samples), validation (5,261 samples) and test data (5,261 samples) in chronological order.

RCF-MNIST [49]: is rotated and colored version of F-MNIST simulating a subpopulation shift. The author rotate the images by a normalized angle $g \in [0, 1]$. In the training data they additionally color 80% of images with RGB values $[g; 0; 1 - g]$ and 20% of images with RGB values $[1 - g; 0; g]$. In the test data, they reverse the spurious correlations, so 80% of images are colored with RGB values $[1 - g; 0; g]$ and the remaining are colored with $[g; 0; 1 - g]$.

Crime [12]: is a tabular dataset combining socio-economic data from the 1990 US Census, law enforcement data from the 1990 US LEMAS survey, and crime data from the 1995 FBI UCR. Each input has 122 features that are supposed to have a plausible connection to crime, e.g. the median family income or per capita number of police officers. The target variable is the per capita violent crimes, representing the sum of violent crimes in the US including murder, rape, robbery, and assault. Following [49], we normalize all numerical features to the range $[0.0, 1.0]$ by equal-interval binning method and we impute the missing values using the mean value of the respective attribute. The state identifications are used as domain information. In total, there are 46 distinct domains and the data is split into disjoint domains. More precise, the training data has 1,390 samples with 31 domains, the validation data has 231 samples with 6 domains and the test data has 373 samples with 9 domains.

SkillCraft [12]: is a tabular dataset originating from a study which uses video game from real-time strategy (RTS) games to explore the development of expertise. Each input has 17 features measuring player-related parameters, e.g. the age of the player and Hotkey usage variables. Following [49], we use the action latency in the game as a target variable. Missing values are imputed using the mean value of the respective attribute. "League Index", which corresponds to different levels of competitors, is used as domain information. In total there are 8 distinct domains and the data is split into disjoint domains. More precise, the training data has 1,878 samples with 4 domains, the validation data has 806 samples with 1 domain and the test data has 711 samples with 3 distinct domains.

DTI [17]: is a tabular dataset where the target is the binding activity score between a drug molecule and the corresponding target protein. The input consists of 32,300 features which represent a one-hot encoding of drug and target protein information. Following [49], we use "Year" as domain information with 8 distinct domains. There are 38,400 training, 13,440 validation and 11,008 test samples.

Methods and Hyperparameters

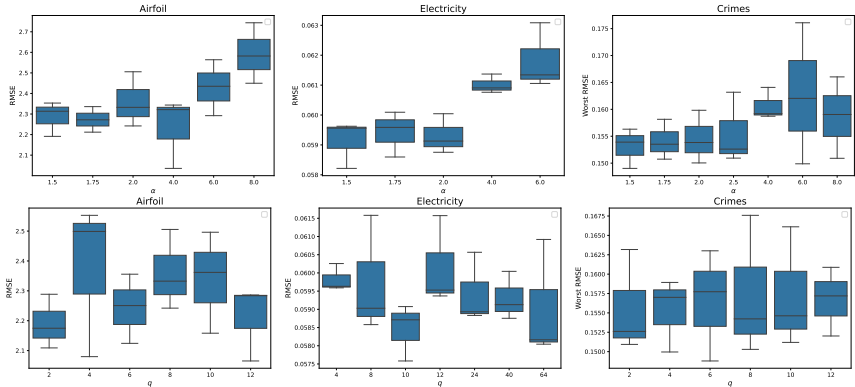
For ERM, Mixup, ManiMixup and C-Mixup, we apply the same hyperparameters as reported in the original C-Mixup paper [49]. According to the authors they are already finetuned via a cross-validation grid search. The details can be found in the corresponding original paper. We rerun their experiments with the provided repository (<https://github.com/huaxiuyao/C-Mixup>) over three different seeds $\in \{0, 1, 2\}$. Furthermore, we finetune ADA and training hyperparameters using a grid search. The detailed hyperparameters for in-distribution generalization and out-of-distribution robustness are reported in Table 3. We apply ADA using the same seeds.

Table 3: Hyperparameters for ADA

	Airfoil	NO2	Exchange	Electricity	RCF-MNIST	Crime	SkillCraft	DTI
Architecture	FCN3	FCN3	LST-Attn	LST-Att	ResNet-18	FCN3	FCN3	DeepDTA
Learningrate	0.01	5e-4	5e-4	5e-4	7e-5	1e-4	0.001	1e-4
Optimizer	Adam	Adam	Adam	Adam	Adam	Adam	Adam	Adam
Batchsize	16	32	64	64	128	48	48	32
Maximum Epoch	200	150	100	100	40	250	100	20
α (determines γ)	2	3.5	1.125	1.125	3	2.5	4	3
Number Groups	8	4	40	40	25	2	16	24
Manifold	1	0	0	0	1	1	0	1

Furthermore, we provide the performance of ADA for different parameter values to get a better understanding of their impact. We vary values for q , the number of clusters used in k-means clustering, and α , the parameter that controls the range of γ -values on selected in-distribution and out-of-distribution datasets. Results are reported in Figure 14.

Figure 14: Results for different α values (upper row) and q values (lower row). Results are reported of three different seeds $\in \{0, 1, 2\}$. For Airfoil and Electricity we report RMSE and for Crimes we report "worst within-domain" RMSE.



Detailed Results

We report the results for in-distribution generalization experiments in Table 4 and for out-of-distribution generalization experiments in Table 5. Following [49], we further evaluated the performance of ADA and C-Mixup on the Poverty dataset [23], which contains satellite images from African countries and the corresponding village-level real-valued asset wealth index. Again we closely followed the experimental setup, so for details we refer to [49]. However, due to computational complexity, ADA hyperparameters are not tuned on this dataset. We use the same learningparameters as reported in [49] and $q = 24$ and $\alpha = 2$.

Table 4: Detailed results for in-distribution generalization. We report the average RMSE and MAPE and the respective standard deviations over three seeds $\in \{0, 1, 2\}$.

	Airfoil				NO2			
	RMSE		MAPE		RMSE		MAPE	
	mean	std	mean	std	mean	std	mean	std
ERM	2.7582	0.1094	1.6942	0.0486	0.5294	0.0128	13.4019	0.3373
Mixup	3.2637	0.1633	1.9645	0.1092	0.5220	0.0037	13.2260	0.1237
ManiMixup	3.0922	0.1668	1.8712	0.0903	0.5277	0.0066	13.3579	0.2148
Local Mixup	3.3727	0.1068	2.0426	0.0211	0.5242	0.0004	13.3087	0.1990
C-Mixup	2.7997	0.2136	1.6289	0.1088	0.5157	0.0123	13.0688	0.3593
ADA	2.3601	0.1339	1.3730	0.0564	0.5147	0.0075	13.1277	0.1468

	Exchange-rate				Electricity			
	RMSE		MAPE		RMSE		MAPE	
	mean	std	mean	std	mean	std	mean	std
ERM	0.0236	0.0065	2.4366	0.7142	0.0582	0.0002	13.9153	0.3410
Mixup	0.0246	0.0058	2.5131	0.6667	0.0581	0.0002	13.8390	0.0539
ManiMixup	0.0246	0.0065	2.5411	0.7417	0.0583	0.0004	14.0308	0.2174
Local Mixup	0.0209	0.0046	2.1360	0.5851	0.0627	0.0054	14.2382	1.2349
C-Mixup	0.0238	0.0061	2.4307	0.6819	0.0573	0.0003	13.5121	0.0979
ADA	0.0209	0.0060	2.1159	0.6889	0.0587	0.0008	13.4642	0.2956

Table 5: Detailed results for out-of-distribution generalization. We report the average and standard deviation of average and worst RMSE or R over three seeds $\in \{0, 1, 2\}$.

	RCF-MNIST		Crime				SkillCraft			
	avg. RMSE		avg. RMSE		worst RMSE		avg. RMSE		worst RMSE	
	mean	std	mean	std	mean	std	mean	std	mean	std
ERM	0.1636	0.0066	0.1356	0.0057	0.1698	0.0066	6.1473	0.4070	7.9064	0.3223
Mixup	0.1585	0.0048	0.1341	0.0031	0.1681	0.0171	6.4605	0.4259	9.8338	0.9415
ManiMixup	0.1572	0.0205	0.1283	0.0030	0.1554	0.0086	5.9080	0.3438	9.2643	1.0117
Local Mixup	0.1873	0.0179	0.1325	0.0033	0.1590	0.0052	7.2514	0.4121	10.9957	0.5702
C-Mixup	0.1579	0.0066	0.1320	0.0017	0.1647	0.0045	6.2156	0.3822	8.2232	0.5463
ADA	0.1629	0.0142	0.1298	0.0032	0.1556	0.0066	5.3014	0.1821	6.8771	1.2666

	DTI				Poverty Map			
	avg. R		worst R		avg. R		worst R	
	mean	std	mean	std	mean	std	mean	std
ERM	0.4827	0.0080	0.4391	0.0154	n/a	n/a	n/a	n/a
Mixup	0.4589	0.0131	0.4239	0.0025	n/a	n/a	n/a	n/a
ManiMixup	0.4736	0.0040	0.4306	0.0087	n/a	n/a	n/a	n/a
Local Mixup	0.4700	0.0127	0.4325	0.0075	n/a	n/a	n/a	n/a
CMixup	0.4735	0.0041	0.4346	0.0082	0.8040	0.0396	0.5388	0.0725
ADA	0.4928	0.0098	0.4483	0.0094	0.7938	0.0328	0.5218	0.0616